VLSI Devices
Lecture 19

Sung-Min Hong (smhong@gist.ac.kr)
Semiconductor Device Simulation Laboratory
Department of Electrical Engineering and Computer Science
Gwangju Institute of Science and Technology (GIST)

Coverage

- Two YouTube lectures reserved for advanced topics
  - L14: ~~Substrate bias~~, ~~channel mobility~~
  - L15: ~~3.2.1~~
  - L16: ~~3.2.1 (Continued)~~
  - L17: Velocity saturation (3.2.2)
  - L18: Channel length modulation and so on (3.2.3, 3.2.4, 3.2.5)
  - L19: MOSFET scaling
  - L20: MOSFET scaling (Continued)
  - L21: Quantum effect (4.2.4)
  - L22: Double-gate MOSFETs (10.3)
  - L23: FinFETs
  - L24: CFETs

Velocity saturation

- Impact of velocity saturation
  - Saturation occurs at a much lower voltage (than $V_{dsat} = (V_{gs} - V_t)/m$).

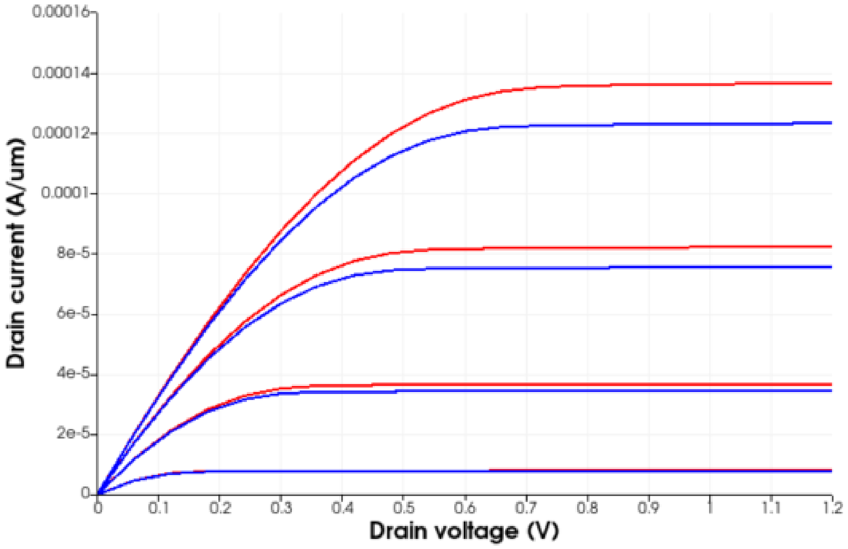

Long-channel

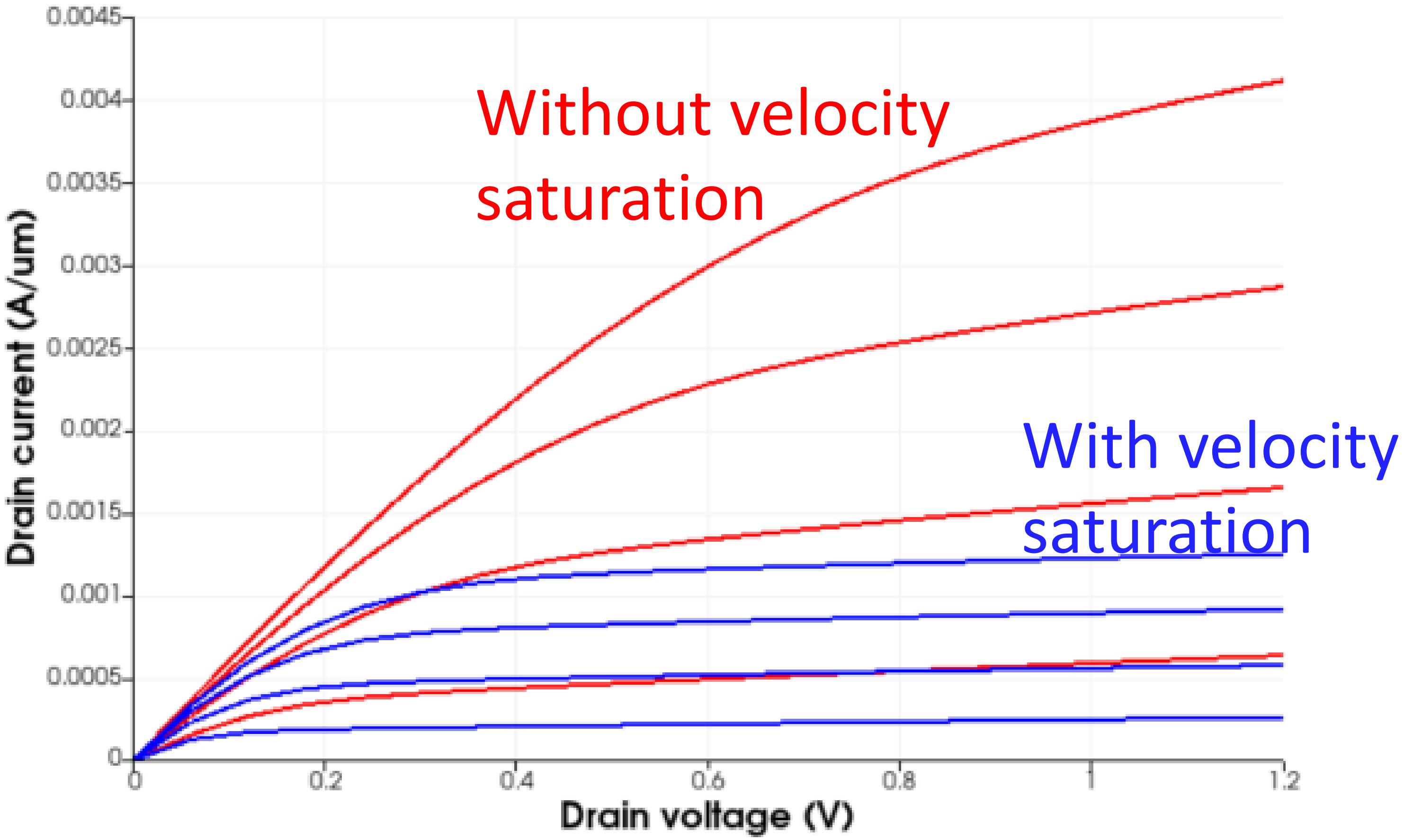

Velocity-field relationship

- Caughey-Thomas
  - Saturation may occur at a much lower voltage (than $V_{dsat} = \frac{V_{gs} - V_t}{m}$).

$$v = \frac{\mu_{eff}\mathcal{E}}{[1 + (\mathcal{E}/\mathcal{E}_c)^n]^{1/n}}$$

Taur, Eq. (3.71)

  - Critical field, $\mathcal{E}_c$
  - For electrons, $n = 2$. For holes, $n = 1$
  - At low fields, $v = \mu_{eff}\mathcal{E}$
  - At high fields ($\mathcal{E} \to \infty$), $v \to \mu_{eff}\mathcal{E}_c = v_{sat}$

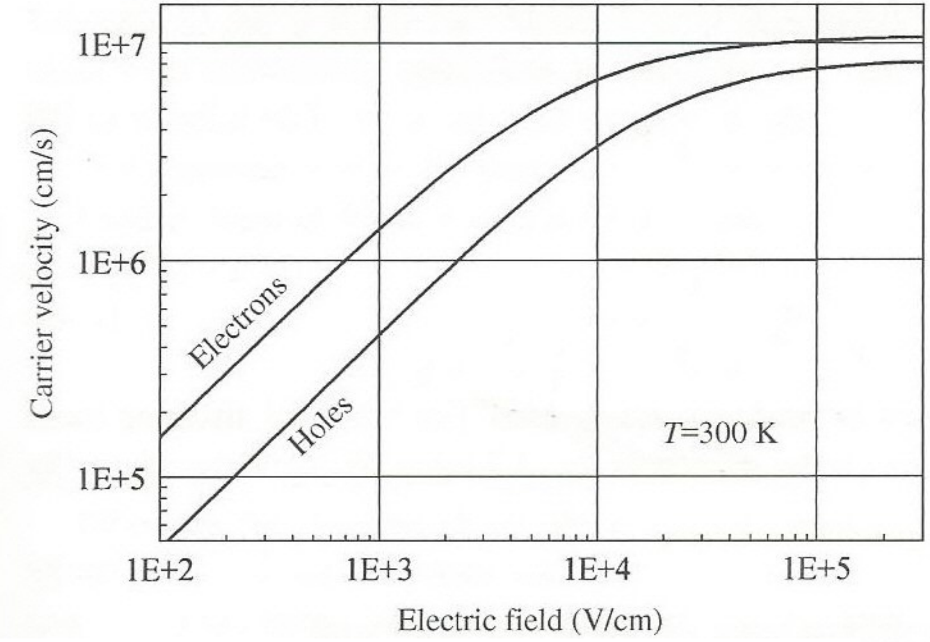

Velocity-field relationship (Taur, Fig. 2.10)

Analytic solution for $n = 1$ (1)

- Valid for holes (PMOSFET)

$$I_d = -WQ_i(V)\frac{\mu_{eff}\dfrac{dV}{dy}}{1+\left(\dfrac{\mu_{eff}}{v_{sat}}\right)\dfrac{dV}{dy}}$$

Taur, Eq. (3.73)

  - Rearranging

$$I_d\left[1+\left(\frac{\mu_{eff}}{v_{sat}}\right)\frac{dV}{dy}\right] = -WQ_i(V)\mu_{eff}\frac{dV}{dy}$$

$$I_d = -\left[\mu_{eff}WQ_i(V)+\left(\frac{\mu_{eff}I_d}{v_{sat}}\right)\right]\frac{dV}{dy}$$

Taur, Eq. (3.74)

Analytic solution for $n = 1$ (2)

- Drain current with velocity saturation

$$I_d dy = -\left[\mu_{eff} W Q_i(V) + \left(\frac{\mu_{eff} I_d}{v_{sat}}\right)\right] dV$$

  - Integration from $y = 0$ to L (from $V = 0$ to V_{ds})

$$I_d L = -\mu_{eff} W \int_0^{V_{ds}} Q_i(V)\,dV - \left(\frac{\mu_{eff} I_d}{v_{sat}}\right) V_{ds}$$

$$I_d L \left(1 + \frac{\mu_{eff} V_{ds}}{v_{sat} L}\right) = -\mu_{eff} W \int_0^{V_{ds}} Q_i(V)\,dV$$

$$I_d = \frac{-\mu_{eff}(W/L) \int_0^{V_{ds}} Q_i(V)\,dV}{1 + \left(\mu_{eff} V_{ds} / v_{sat} L\right)}$$

Taur, Eq. (3.75)

Analytic solution for $n = 1$ (3)

- Using the chage-sheet model

$$Q_i = -C_{ox}\left(V_{gs} - V_t - mV\right)$$

Taur, Eq. (3.76)

$$I_d = \frac{\mu_{eff} C_{ox}(W/L)\left[\left(V_{gs} - V_t\right)V_{ds} - \frac{m}{2}V_{ds}^2\right]}{1 + \left(\mu_{eff} V_{ds}/v_{sat}L\right)}$$

Taur, Eq. (3.77)

- By solving $\frac{dI_d}{dV_{ds}} = 0$ at V_{dsat},

$$0 = \frac{\left(V_{gs} - V_t\right) - mV_{dsat}}{1 + \left(\mu_{eff} V_{dsat}/v_{sat}L\right)} - \frac{\left(V_{gs} - V_t\right)V_{dsat} - \frac{m}{2}V_{dsat}^2}{\left[1 + \left(\mu_{eff} V_{dsat}/v_{sat}L\right)\right]^2}\left(\mu_{eff}/v_{sat}L\right)$$

Analytic solution for $n = 1$ (4)

- Manipulation

$$\left[\left(V_{gs}-V_t\right)-mV_{dsat}\right]\left[1+\left(\mu_{eff}V_{dsat}/v_{sat}L\right)\right]$$
$$=\left[\left(V_{gs}-V_t\right)V_{dsat}-\frac{m}{2}V_{dsat}^2\right]\left(\mu_{eff}/v_{sat}L\right)$$

$$V_{dsat}=\frac{2\left(V_{gs}-V_t\right)/m}{1+\sqrt{1+2\mu_{eff}\left(V_{gs}-V_t\right)/(mv_{sat}L)}}\le\left(V_{gs}-V_t\right)/m$$

Taur, Eq. (3.78)

$-L\rightarrow\infty, V_{dsat}=\left(V_{gs}-V_t\right)/m$

$-L\rightarrow 0,$

$$V_{dsat}=\sqrt{\frac{2\left(V_{gs}-V_t\right)v_{sat}L}{\mu_{eff}m}}$$

Analytic solution for $n = 1$ (5)

- Two extreme cases
  - $L \to \infty$,

$$I_{dsat} = \mu_{eff} C_{ox} \frac{W}{L} \frac{\left(V_{gs} - V_t\right)^2}{2m} \qquad \text{Taur, Eq. (3.80)}$$

  - $L \to 0$,

$$I_{dsat} = C_{ox} W v_{sat} \left(V_{gs} - V_t\right) \qquad \text{Taur, Eq. (3.81)}$$

  - In this case, I_{dsat} is independent of channel length L and varies linearly with $V_{gs} - V_t$ instead of quadratically as in the long-channel case.

Other case, $\boldsymbol{n = \infty}$ (1)

- We are more interested with n = 2.
  - Although details are different, different models share two extremes:
  - $L \to \infty$,

$$I_{dsat} = \mu_{eff} C_{ox} \frac{W}{L} \frac{\left(V_{gs} - V_t\right)^2}{2m} \qquad \text{Taur, Eq. (3.80)}$$

  - $L \to 0$,

$$I_{dsat} = C_{ox} W v_{sat} \left(V_{gs} - V_t\right) \qquad \text{Taur, Eq. (3.81)}$$

Velocity overshoot

- 70-nm-long double-gate MOSFET
  - Strong velocity overshoot

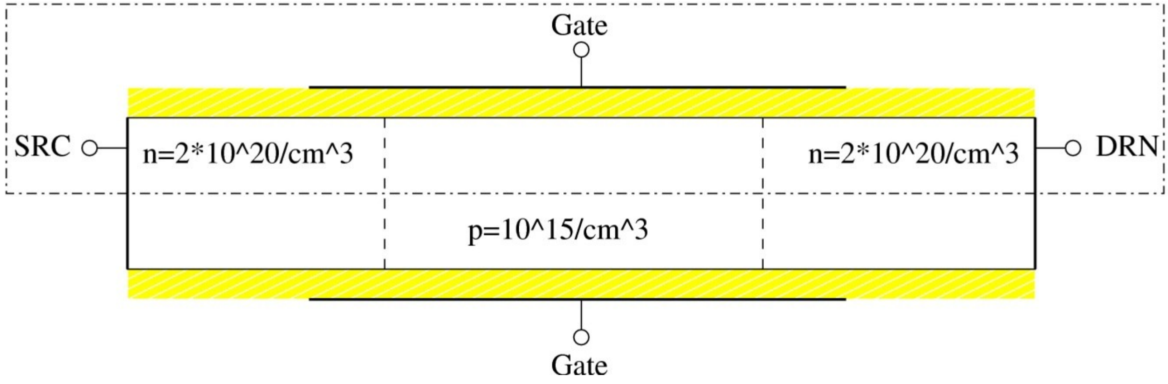

V_{ds} = 0.9 V

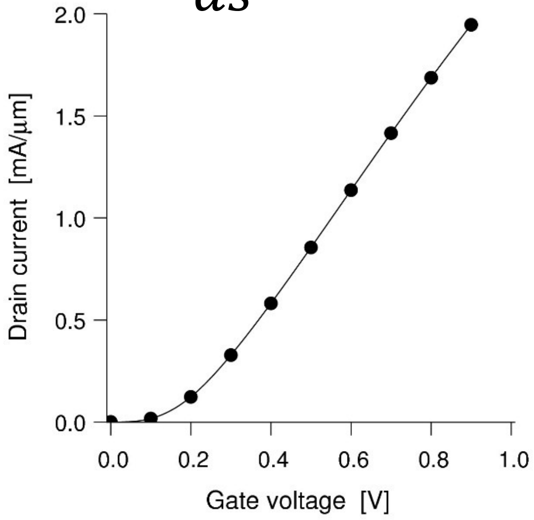

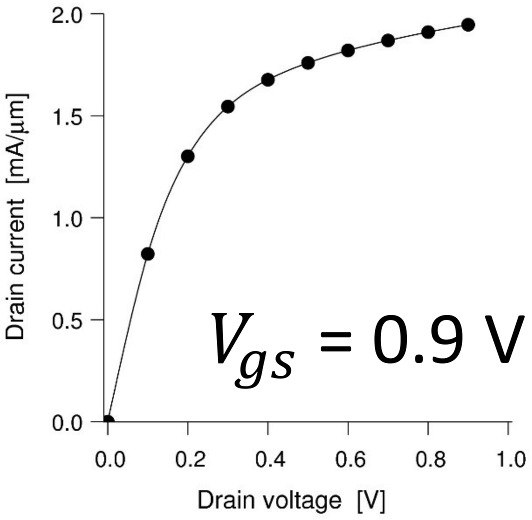

V_{gs} = 0.9 V

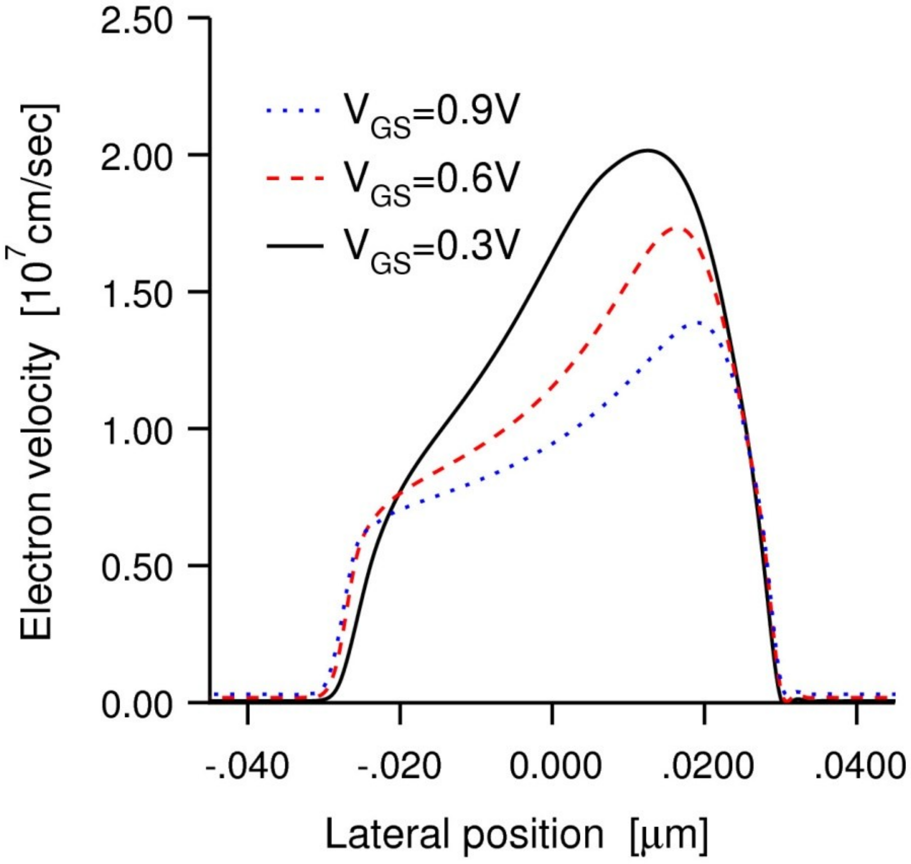

Channel length modulation

- Gradual-channel approximation fails at the saturation point.
  - Distance between the saturation point and the drain, ΔL.
  - Drain current increases as

$$I_d = \frac{I_{dsat}}{1 - (\Delta L / L)}$$

Taur, Eq. (3.101)

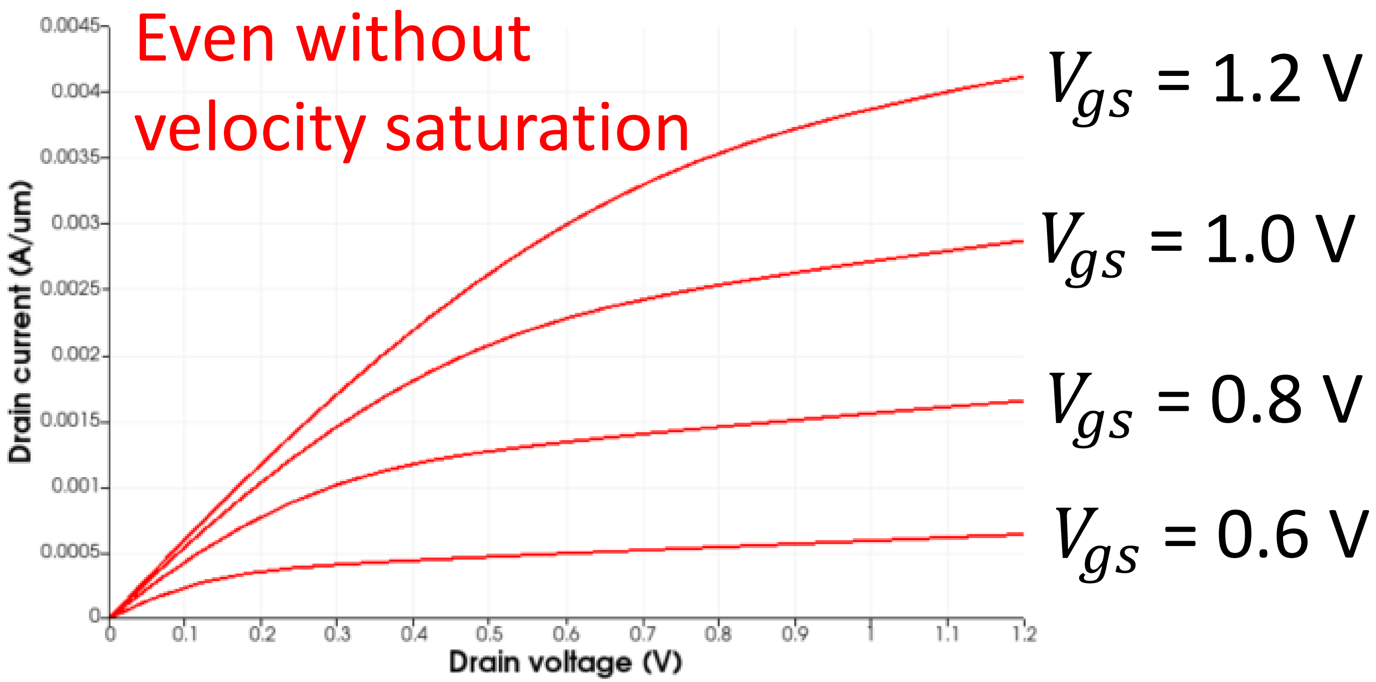

Case study: TSMC 3 nm node

- IEDM 2022 (27.1)
  - DIBL versus L

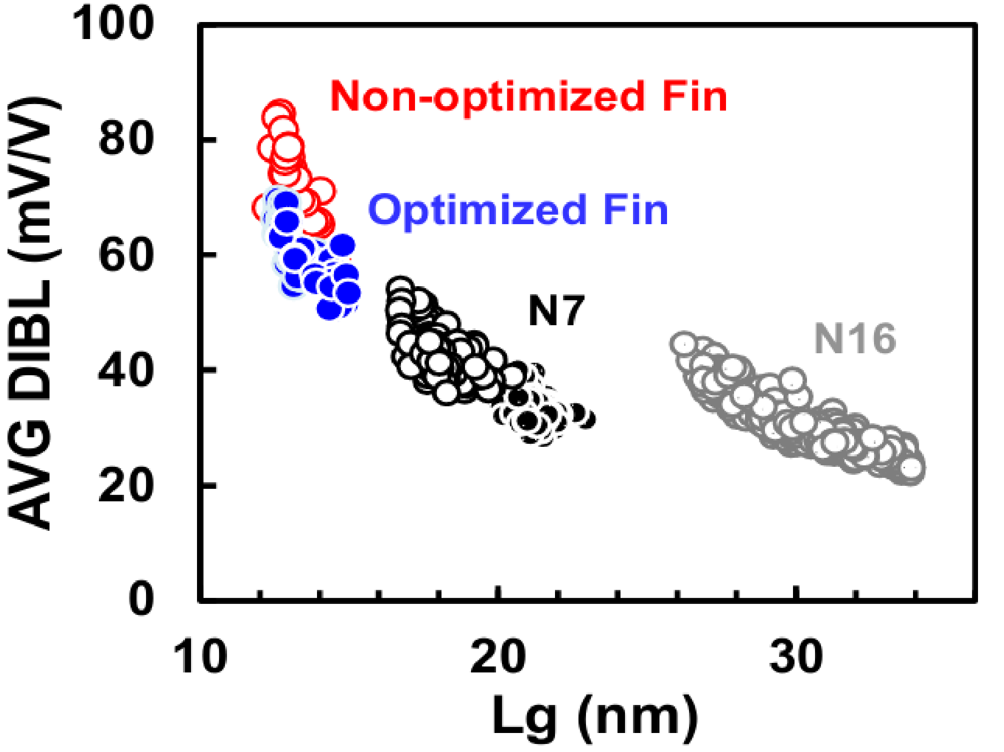

Fig.1 FinFET Lg scaling trend vs DIBL. Fin profile optimization is critical but is at the limit for further Lg scaling.

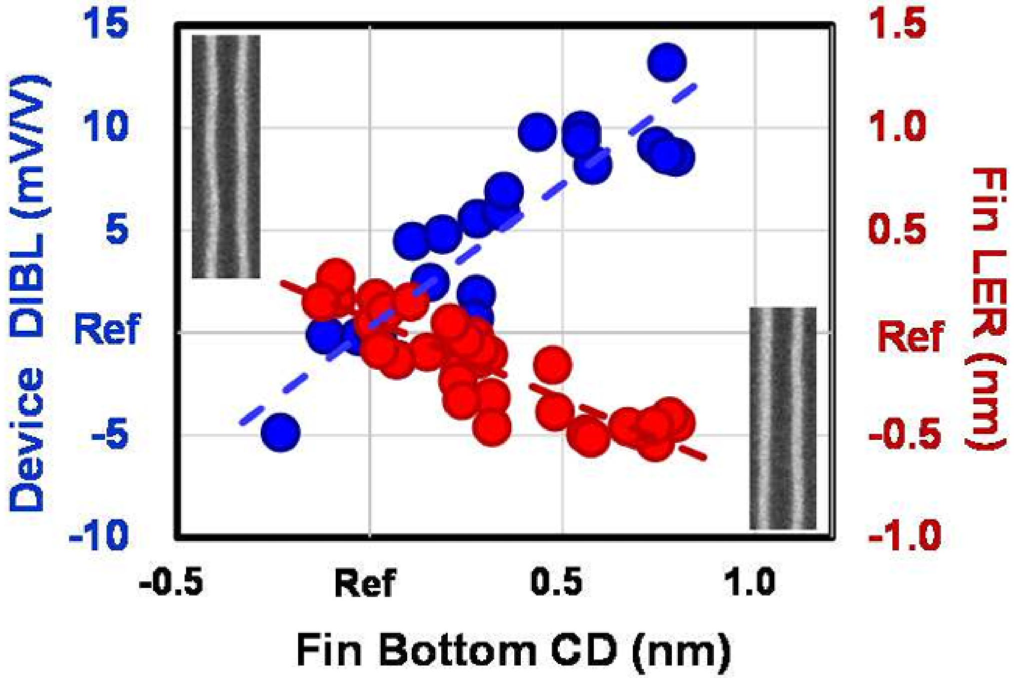

Fig.2 Smaller fin bottom CD reduces DIBL but degrades LER, which is an indicator of fin structural robustness and potential yield impact.

Source-drain series resistance

- Finite silicon resistivity + metal contact resistance
  - MOSFET channel resistance in the linear region

$$R_{ch} = \frac{V_{ds}}{I_d} = \frac{L}{\mu_{eff} C_{inv} W (V_{gs} - V_{on})}$$

Taur, Eq. (3.102)

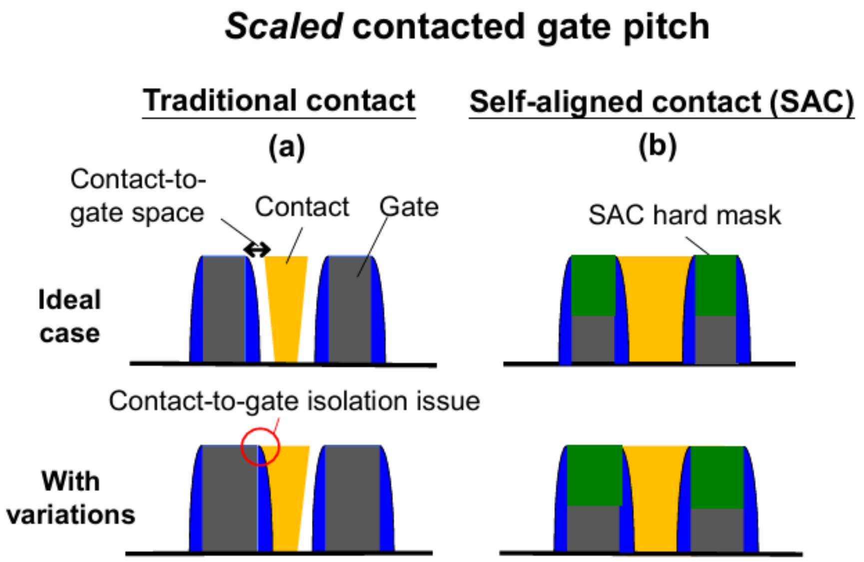

Fig.3 Contact schematics. Traditional contact (a) is vulnerable to variations induced contact-to-gate isolation issues compared to SAC (b).

Self-aligned contact (TSMC, IEDM 2022)

Thank you!